Journal of Non-Crystalline Solids 444 (2016) 49–54

Contents lists available at ScienceDirect

Journal of Non-Crystalline Solids

journal homepage: www.elsevier.com/locate/jnoncrysol

Dielectric relaxation of vanadium–molybdenum tellurite glasses modified by alkaline-earth oxides

S. Terny [a,b], P.E. di Prátula [a], J. De Frutos [b], M.A. Frechero [a,*]

[a] INQUISUR, CONICET, Departamento de Química, Universidad Nacional del Sur (UNS), Av. Alem 1253, 8000 Bahía Blanca, Argentina
[b] POEMMA-CEMDATIC, E.T.S.I. Telecomunicación, UPM, Avda. Complutense, 30, 28040 Madrid, Spain

ARTICLE INFO

Article history:
Received 18 February 2016
Received in revised form 19 April 2016
Accepted 22 April 2016
Available online 7 May 2016

Keywords:
Oxide glasses
Impedance spectroscopy
Electrical properties
Ionic conductivity
Dielectric properties

ABSTRACT

Electrical response changes due to the incorporation of alkaline-earth oxides in the vanadium–molybdenum tellurite glassy matrix have been studied. The results are explained by analyzing the electric formalisms representations. A non-straightforward relationship to the modifier oxide ionic radius was found and the results suggest poor charge carrier interactions even at high alkaline-earth concentrations. The electrical behavior of the studied materials gives strong evidence that alkaline-earth modified tellurite glasses are poor candidates to become good ionic glassy conductors.

1. Introduction

In 1998, C.T. Moynihan had showed that the use of the electric modulus M* in analysis of electrical responses in ionically-conducting glasses is useful because it allows a comparison between electrical relaxation results and structural relaxations results [1]. When one discusses the electrical response of ionic conductors, it is necessary to make a distinction between relaxation and dispersion as J.R. Macdonald highlighted in his review in 2010, he distinguishes between a dispersion of dielectric relaxation times (Debye's response contains a single time constant) and resistive relaxation times (which consist of a discrete or continuous distribution of relaxation times) that involve mobile charges [2].

Electrical measurements in ionic glasses are very useful to carry out in a frequency domain. In general, what is measured is the parallel conductance (G) and the capacitance (C) of the sample using an admittance bridge or the magnitude of the sample impedance |Z| and the phase angle ϕ, using an impedance meter. Usually, those results are expressed in terms of complex permittivity (ε^*) or the complex conductivity (σ^*) which are related by the following expression:

$$\sigma^* = i\omega\varepsilon_0\varepsilon^* \tag{1}$$

where ε_0 is the permittivity of vacuum, ω is the angular frequency and i is the imaginary unity.

Two characteristic properties of a material, definable in terms of the quantities presented in Eq. (1) are: the dc electrical conductivity which involve the long range displacement of mobile ions, σ_{dc} (when $\omega \to 0$); and the high frequency dielectric constant, ε_∞ (when $\omega \to \infty$).

However, nowadays, analysis of such data tends to focus on the frequency dependence of either the real part of the conductivity or of the complex modulus. The electric modulus formalism, M*, was firstly developed by Macedo et al. [3,4] to consider the electrical response as a function of frequency, in an analogous manner to the mechanical shear stress relaxation in liquids, where a system initially in equilibrium is perturbed. The kinetics of its approach to a new equilibrium state is described in terms of a relaxation function in the time domain $\phi_{(t)}$. In the time domain, the relaxation (to zero at long times) of the electric field $\mathbf{E}_{(t)}$ in an ionic conductor under the constrain of the constant displacement vector **D** imposed at time zero is given by:

$$\mathbf{E}_{(t)} = E(0)\int_0^\infty g_{(\tau)} \cdot \exp\left(-\frac{t}{\tau}\right) d\tau \tag{2}$$

where $\phi_{(t)}$ is the electric field relaxation function, τ an electric field relaxation time and $g_{(\tau)}$ is the normalized probability density function for τ.

In the frequency domain, the corresponding electric field relaxation is described in terms of the electric modulus M*:

$$M^* = M' + iM'' = M_\infty \int_0^\infty g_{(\tau)} \left[\frac{i\omega\tau}{(1+i\omega\tau)}\right] d\tau. \tag{3}$$

* Corresponding author.
E-mail address: frechero@uns.edu.ar (M.A. Frechero).

http://dx.doi.org/10.1016/j.jnoncrysol.2016.04.041
0022-3093/

The time scale for the electric field relaxation is parameterized by mean relaxation time $\langle\tau\rangle$, whose value is in turn given by:

$$\tau = \int_0^{\infty} g_{(\tau)}\tau d\tau = \varepsilon_0\varepsilon_\infty/\sigma = \frac{\varepsilon_0}{M_\infty}. \quad (4)$$

Most of the relaxation of the electric field is expected to occur at frequencies in the vicinity of the frequency where $\omega \cdot \langle\tau\rangle = 1$. This characteristic frequency corresponds closely to the frequency of the maximum in M″ and to the frequency range where M′ changes more rapidly.

The most important feature of electrical relaxation data analysis for conducting glasses, which focuses on frequency dependence of σ′, is often given a very literal interpretation: a measure of the flux of electrical charge due to the motion of mobile charge carriers (ions, polarons or both) [5]. However, if a whole analysis of the electrical relaxation behavior of the system is done from the electric formalisms for description of electrical relaxation data it is possible to understand, more deeply, the way that the system responds to an applied external electrical field. More than that, the change on the electrical response induced by the presence of different modifier oxides in the glassy matrix is done more obvious. Because of this, we present here our results in such a comparative way in order to show the differences provoked by four alkaline-earth oxides on the same tellurite glassy matrix. A priori, the only property that is changed is the alkaline-earth cation radius (Mg: 0.60 Å; Ca: 1.00 Å; Sr: 1.20 Å; Ba: 1.40 Å) [6]. The general formula of the glassy system studied in this work is: xMO$(1-x)$[0.5$V_2O_5$0.5MoO_3]2TeO_2 with M = Mg, Ca, Sr or Ba which allow us to focus only on the modifier oxide cation. For the sake of clarity we have emphasized on some figures the results of samples with the lowest and highest modifier oxide content. The obtained results show that other properties of the modifier oxide than their cation radius is involved in the electric response of these glasses and we argue about those.

2. Experimental

The samples of this work of general formula: x**M**O$(1-x)$[0.5$V_2O_5$0.5MoO_3]2TeO_2 (**M** = Mg, Ca, Sr, Ba) were prepared by a standard melt quenching technique starting from reagent grade chemicals of TeO_2, MoO_3, V_2O_5, $MgCO_3$, $CaCO_3$, $SrCO_3$ and $BaCO_3$. Appropriate amounts of the components were well mixed and placed in an alumina crucible. Next, the carbonate decarboxylation process was made at a lower temperature than the mix melting point. When the effervescence finished, the mix was heated to reach a temperature of 1373 K in an electric furnace for 1 h. During the process, the crucible was shaken frequently to ensure homogenization. After this procedure the molten material was poured onto a preheated aluminum plate in form of drops and held at 250 °C during 2 h for annealing.

The amorphous character of the samples was tested by X-ray diffraction (XRD) analysis. The X-ray diffraction patterns of powdered samples after the annealing were collected with a Bruker D8 Advance diffractometer in continuous scan mode with a copper anode and 45 kV–30 mA for the tension and electrical current generator respectively. The samples were exposed to the Cu K_α radiation (λ = 1.54 Å) at room temperature in the 2θ range: 10°–60°.

Differential Scanning Calorimetry (DSC) curves were recorded during heating rate a 10 K min^{-1} using a SDT-Q600 in order to find the glass transition temperature (T_g) of each sample starting from room temperature up to 600 °C and using 15–20 mg of glass samples previously milled in an agate mortar. Each value of T_g is obtained from the middle point of the C_p jump during the heating. The associated upper limit error of the temperature measurements is one degree according to the middle point procedure with the TQA software.

In order to obtain the electrical characterization of our materials, the samples were polished with very fine sand papers to obtain glass disks with two parallel faces of thickness ranging between 0.5 and 0.7 mm. Each sample was coated uniformly with a thin layer of silver paint with the purpose of having proper electrical contact. For the impedance determinations, Impedance/Gain-phase Solartron analyzer with 1296 a dielectric measuring module, which allows analysis within the range of frequencies from 10 μHz to 10 MHz, of 10^2 to 10^7 Ω impedances. To do the analysis of the results has been used the Solartron ZPlot software package. The measured were carried out at V_{AC} = 0.80 V, in a frequency range of [10^{-2}–10^6] (only for barium oxide modified system the impedance measurements were carried out with an Agilent 4284A LCR meter in frequency range from 20 Hz to 1 MHz). For each composition the spectra were carried out in a temperature range starting at 100 °C up to a temperature 15 °C below its T_g to avoid sample structural changes.

Density measurements were done following the Archimedean's method using distilled water as secondary displacement medium. In order to obtain the average density values, three independent measurements were carried out per composition.

3. Results and discussion

Fig. 1 shows the X-ray diffraction patterns. The base line deviation intensity in the pattern (in the range from 20° to 30° 2θ degrees) is smooth and do not present sharp peaks. From these results we assume that every sample is a glass material.

Fig. 2a shows the corresponding T_g as a function of x (alkaline-earth content) for every studied glass system. From this figure, we learn that T_g values increases between 20% and 50% depending on the alkaline-earth oxide. This behavior is the opposite of that observe when the modifier oxide is an alkaline oxide (T_g decreases when the alkaline oxide content increases in this type of glassy matrix) [7].

Fig. 2b shows the corresponding T_g as a function of radius modifier cation. There is not a direct correlation between the cation modifier radius with the of the T_g value. According to N.H. Ray [8], the transition temperature of an oxide glass increases with the cross-link density of the network caused by the strength of the bonds it is composed of and the tightness of its packing in the network. Also, they mention that, in general, the cross-linking has a greater effect than the bond strength. Considering this explanation from this Fig. 2b we learn that Sr^{2+} has the better size to this type of glassy matrix while to reach a similar effect with Mg^{2+} is needed larger quantity of MgO. Ca^{2+} and Ba^{2+} do not fit very well and do not reach the same behavior even they induce the necessary cross-linking to increases the T_g. Fig. 2c gives the tree properties simultaneously: cation radius vs. cation modifier content vs. T_g and it shows clearly that there is not a direct and unique relationship among them.

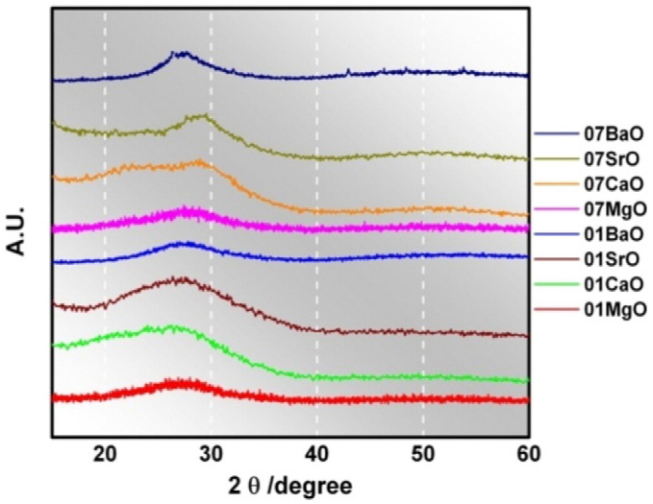

Fig. 1. X-ray diffraction patterns of the studied systems.

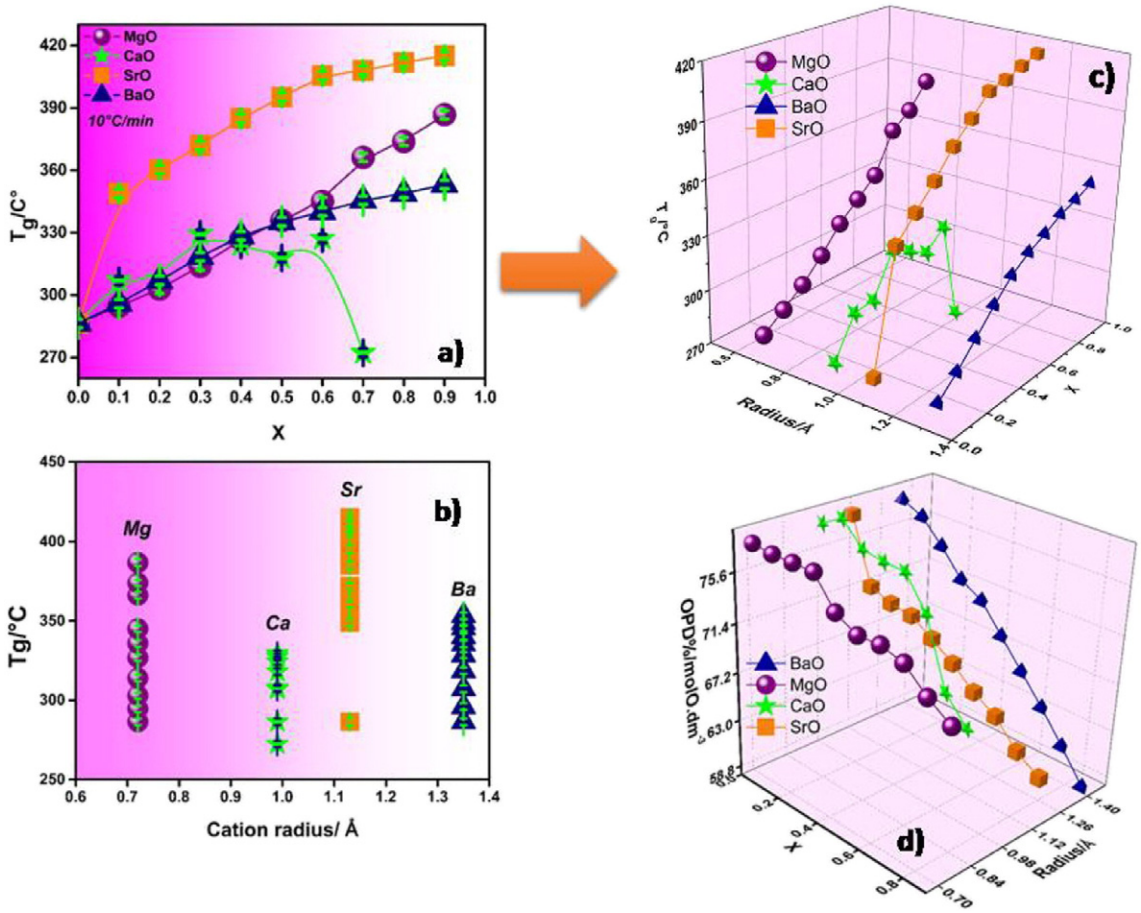

Fig. 2. a) T_g as a function of alkaline-earth content (x); b) T_g as a function of radius modifier cation; c) Comparison of: cation radius vs cation modifier content vs T_g; d) Comparison of: cation radius vs cation modifier content vs OPD (every line was drawn as guide to the eye).

Fig. 2d shows the oxygen packing density. Considering a glass as a three dimensional framework of connected oxygen-tellurium polyhedra mainly by covalent bonds, the oxygen packing density (OPD: the number of mol of oxygen atoms per dm^3 of glass) becomes a relevant magnitude to analyze the compactness of the structure and the variations on it provokes by a modifier oxide, in this work, the alkaline-earth oxides. Density values are listed in Table 1. In this Fig. 2d, we observe that the OPD decreases continuously when x goes from $x = 0.0$ to $x = 1.0$ where the packing diminishes when x increases. From this figure we learn that the alkaline cation size makes evident, as the cation is larger the compactness of the glassy matrix is lower. The OPD variation forces the network to a strong rearrangement in the spatial distribution of the polyhedron that builds it.

Table 1
Density values of every studied system.

x	[Density ± 0.01] g·cm^{-3}			
	MgO	CaO	SrO	BaO
0.0	4.67	4.67	4.67	4.67
0.1	4.72	4.81	4.45	4.79
0.2	4.78	4.77	4.53	4.85
0.3	4.85	4.84	4.64	4.89
0.4	4.78	4.93	4.71	5.02
0.5	4.80	4.86	4.77	5.08
0.6	4.89	4.59	4.82	5.13
0.7	4.95	4.55	4.91	5.28
0.8	4.94	–	4.95	5.25
0.9	4.96	–	5.06	5.30

We see now how every structural feature that we have presented before manifests itself on the electrical behavior of the studied glasses in the present work. Fig. 3 shows the real part of the complex conductivity spectra for the systems with low and high alkaline-earth oxide concentration in a similar temperature range. This is a well established method for characterizing the hopping dynamics of charge carriers [9,10]. The electrical response shows significant changes between concentrations in both extremes ($x = 0.1$ vs $x = 0.7$), not only in their magnitudes but also in their spectrum shapes. For all the $x = 0.1$ compositions, the plateau corresponding to σ_{dc} is observed over six orders of log[freq] (or even more, depending on the temperature) in the range of the lower frequencies. While for the $x = 0.7$ compositions their spectra are quite noisy and very dissimilar among the set of alkaline-earth modifier oxides studied (Mg, Ca, Sr, Ba). Additionally, if we pay attention to the high frequency range, the differences are even stronger than the ones observed at low frequencies. All the compositions with a lower modifier oxide content show harder conductivity temperature dependence, while those with a higher modifier oxide content show a weaker or almost imperceptible dependence. But, we observe a significant difference in the conductivity slope at high frequency. While for the Ca^{2+} samples, the slope is of around one, for larger cations, the slope decreases. This is a signature of ion interaction or cooperative mechanism [11,12]. We leave the Mg^{2+} sample out in the present discussion because, as we demonstrated in a previous work [13,14,15], that system never reaches ionic conductivity and in the whole range of modifier oxide content studied, Mg^{2+} does not move freely in this tellurite glassy matrix so as a result the electrical response is only due to polarons.

We see in the imaginary part of the dielectric constant in Fig. 4 that it does not show a direct relationship with the cation radius. One more

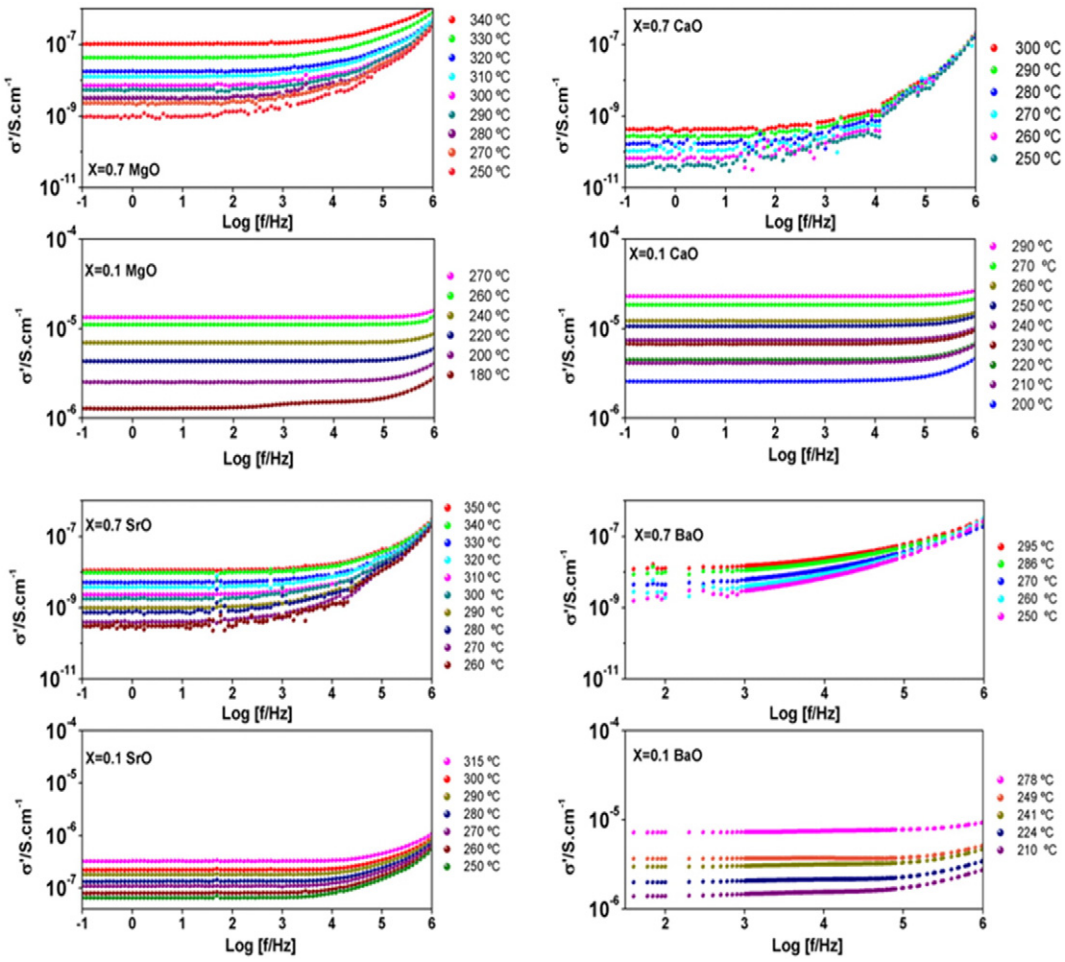

Fig. 3. Spectra of the real part of complex conductivity at a similar temperature range for low and high alkaline-earth content.

time, as in the conductivity spectra, the strontium's behavior is very different among other alkali-earth oxides.

Loss peaks are not observed in Fig. 4 for compositions with low alkaline-earth oxide content ($x = 0.1$). Nevertheless, for high content modifier oxides ($x = 0.7$) an incipient loss peak seems to appear at a high frequency (above 10^5 Hz). However, this is less clear when the modifier oxide corresponds to the largest cation (Ba^{2+}). We notice in this figure that all the compositions with $x = 0.7$ reach lower values at each frequency compared to its respective $x = 0.1$ (about four orders of magnitude). However, when the modifier oxide is SrO, its behavior is quite different. For $x = 0.7$, ε'' value is similar to the composition modified with CaO while for $x = 0.1$ of SrO its ε'' value is two orders of magnitude lower. Because of the permittivity data is not enough to obtain information about the relaxation time distribution behavior [16], as we have discussed previously, the electric modulus M* corresponds to the relaxation of the electric field in the material when the electric displacement remains constant. This spectrum allows us to obtain information about the relaxation mechanism when the dielectric loss peak is not clear enough on their spectra. The frequency dependence of the calculated real ($M'_{(f)}$) and imaginary ($M''_{(f)}$) parts of the electric modulus are shown in Figs. 5 and 6 for a selected temperature of each studied system. In Fig. 5 we see that $M'_{(f)}$ curves tend towards zero at low frequencies and to a frequency-independent constant at high frequencies, indicating that the initial dispersion in M' and M'' are due to a conductivity relaxation [17]. The fact, that M' approaches zero at low frequencies also indicates that electrode polarization has a negligible effect on data analysis in modulus notation. The $M''_{(f)}$ curves in Fig. 6 are very symmetrical and show the presence of only one relaxation process and the maximum of symmetric peaks shifts towards lower frequencies when the alkaline oxide content is high. Once again, $x = 0.1$ of SrO has a different behavior than the other alkaline-earth oxides, its $M''_{(f)}$ maximum is observed at a lower frequency, about two orders of magnitude.

The temperature dependence of dc conductivity shown in Fig. 3 is well described by the Arrhenius law that reflects the thermally activated hopping process for each composition. The activation energy of the charge carrier hopping for each of the compositions obtained from the

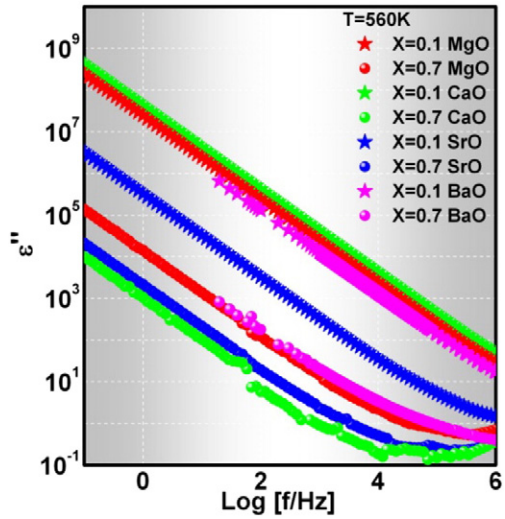

Fig. 4. Imaginary part of dielectric constant as a function of frequency at 560 K.

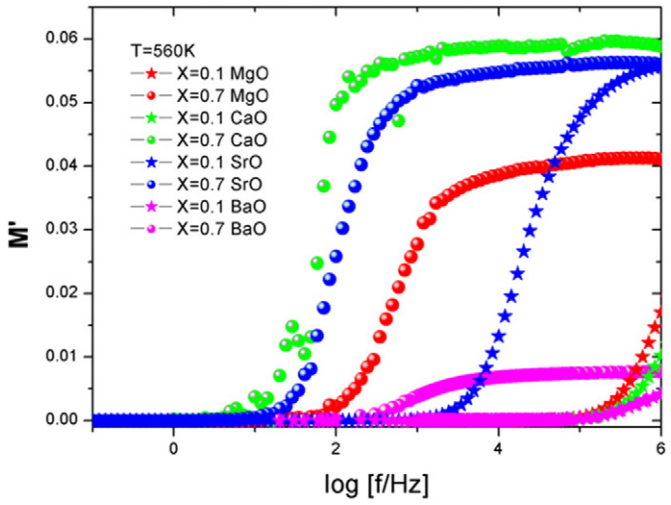

Fig. 5. Frequency dependence of M'_{ω} at 560 K.

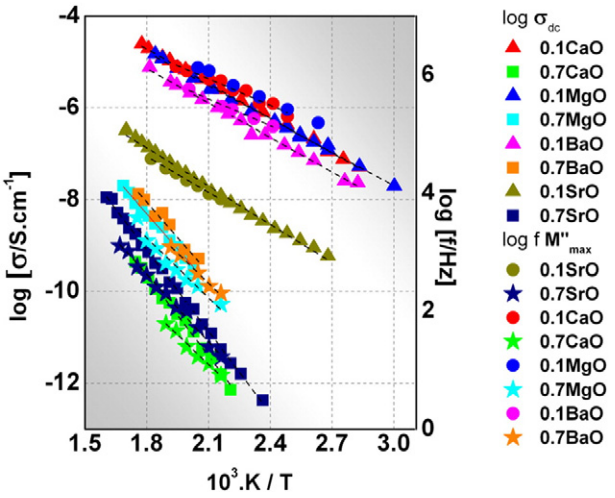

Fig. 7. Temperature dependence of dc conductivity and relaxation frequency (τ^{-1}) obtained from the M''_{max} (dotted lines corresponding to linear regression fit with a $R^2 = 0.99$).

slops in Fig. 7 is plotted in Fig. 8 as a function of the alkaline-earth cation radius.

Considering that the ion or polaron hopping ac conductivity can be expressed by the Fourier transform of the time derivative of $\Phi(t)$ [18,19,20].

$$\sigma^*(\omega) = \frac{1}{\varepsilon_\infty}\left[1 - \int_0^\infty \left(-\frac{d\varphi}{dt}\right) e^{-j\omega t} dt\right] \quad (5)$$

which is reasonably fitted to the Kohlrausch stretched exponential relaxation function of the form: $\Phi(t) = \exp(-(t/\tau)^{1-n})$ with $0 < (1-n) \leq 1$. The characteristic relaxation time τ is found to be thermally activated with the activation energy of the dc conductivity. The Coupling Model (CM) [8,21,22,23] accounts for the stretched exponential time dependence of the relaxation function as a consequence of the cooperativity among the charge carriers (ions or polarons) in the particle diffusion process [24]. Initially, it starts with independent hops of carriers to neighboring available site with an exponential correlation function: $\Phi(t) = \exp(-t/\tau_0)$ whose relaxation time is τ_0. Such independent hops cannot occur for all carriers at the same time because of their interactions and correlations. Those interactions are responsible for the slowing down of the relaxation rate at longer times and because of this, the correlation function changes from a Deby's type to the Kohlrausch function, where n is a measurement of the cooperative effects. A major result of the CM is that the effective relaxation time τ is related to τ_0 by:

$$\tau = \left[t_c^{-n}\tau_0\right]^{1/(1-n)}. \quad (6)$$

For charge carriers vibrating in their cages and hopping to neighboring sites through barriers of energy E_a, the relaxation time for independent hopping is: $\tau_0(T) = \tau_\infty \exp(E_a/kT)$. The reciprocal of τ_∞ is the attempt frequency of the charge carrier. Then, we can see that the activation energy for the dc conductivity or τ could be larger than that energy barrier given by the relationship:

$$E_{dc} = E_a/(1-n). \quad (7)$$

The increase of the interaction magnitude leads to a higher degree of cooperativity in the hopping process, which corresponds to a higher value of the coupling parameter n and consequently, higher activation energy for long-range ionic transport [25]. Then, from our results presented in Figs. 7 and 8, we assume that the interactions among charge carriers are poor (as it was expected from the shape of $M''_{(f)}$ curves).

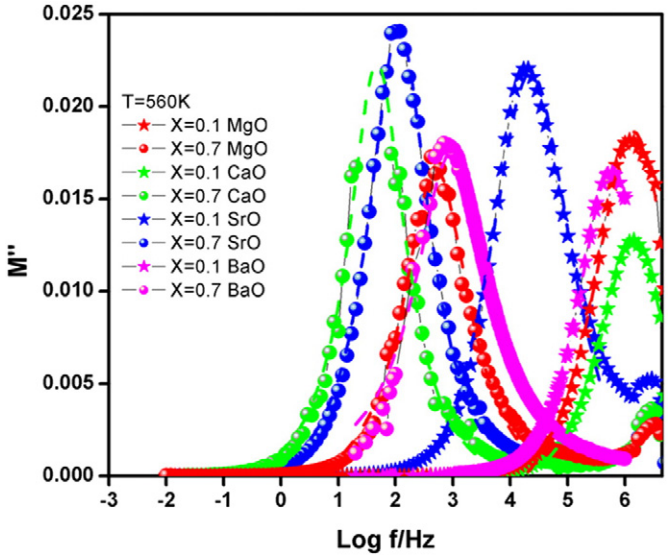

Fig. 6. Frequency dependence of M''_{ω} at 560 K (every line was drawn as guide to the eye).

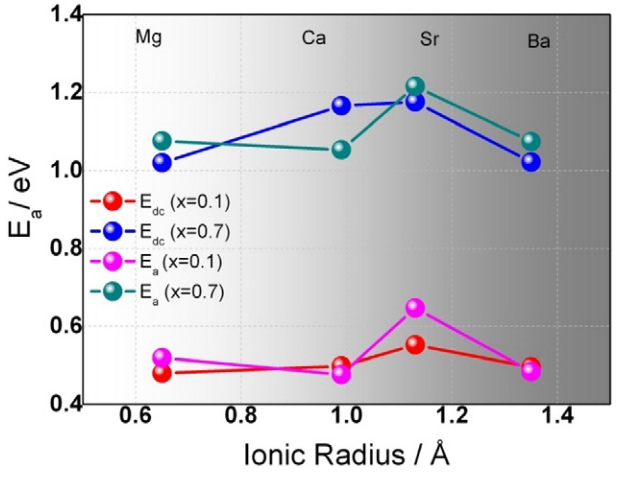

Fig. 8. Activation energy (E_a and E_{dc}) as a function of the alkaline-earth cation radius (every line was drawn as guide to the eye).

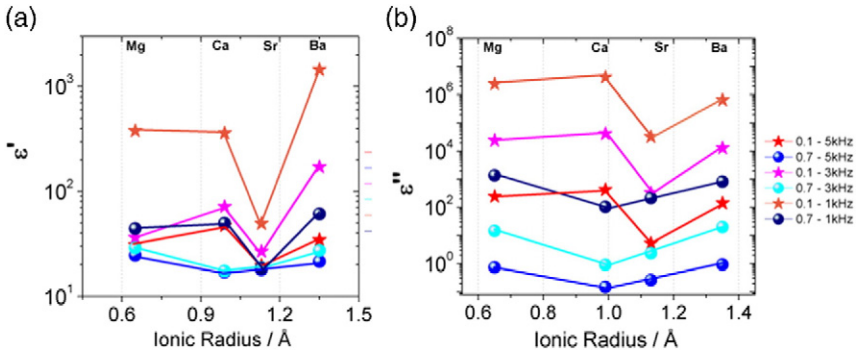

Fig. 9. a) Real part and b) imaginary part of selected frequency values at 560 K (every line was drawn as guide to the eye).

In order to make a comprehensive analysis among the set of alkaline-earth modifier oxides, we plot in Fig. 9a and b the real and imaginary part of ε*, for selected values of the frequency (the highest frequency is in the range where the conductivity is frequency dependent; the intermediate frequency is in the transition to the dc conductivity and the lowest frequency belongs to the range where dc conductivity is clear observed).

It is clear in these figures that the change on ε* does not show a monotonous behavior when the alkaline-earth radius cation varies. But, it is worth to note that for low ($x = 0.1$) alkaline-earth oxide content SrO has the most different behavior. For all the frequencies plotted here that composition reaches the lowest values in both real and imaginary components. For high ($x = 0.7$) alkaline-earth oxide content a minimum in ε″ appear in the composition modified with CaO. But, ε′ shows a random behavior.

Then, as we proposed in the Introduction section, this work has not found a straightforward relationship between the changes in the electrical response of this Tellurite glass and the ionic radius of the modifier oxide incorporated (as the expected behavior induced by modifier alkaline oxides, something that has been extensively discussed elsewhere) [26,27,28,29,30,31,32,33].This is a result that forces us to rethink the common expression for ionic conductivity: $\sigma = q \cdot N \cdot \mu$ (carrier charge; carrier concentration; carrier mobility); in which we assume that univalent and bivalent cations have the same behavior.

4. Conclusions

The main result of the present work is that a non-straightforward relationship between the modifier oxide ionic radius and the electrical behavior is observed in tellurite-vanadium glassy matrices. Additionally, has been evidenced a weak charge carrier interaction in the conductivity spectra of each of the bivalent cations studied here (Mg, Ca, Sr, Ba). The whole comparative studied of alkaline earth modified oxides as modifier oxides in this Tellurite Vanadium glassy matrix gives strong evidence that they are not appropriated candidates to become ionic glassy conductors in order to be able of transport charge, i.e. good ionic conductors. However, it is necessary to studied in more detail the peculiar behavior of the SrO which suggest that interact with the glassy matrix differently to the other alkaline earth oxides.

Acknowledgement

This work has been possible to the financing of the Spanish MINECO (project MAT2013-48009-C4-3-P), ARCOIRIS ERASMUS MUNDUS ACTION 2 Lot 16A (Argentine). Financial support by CONICET (PIP 013-2015GI) and Universidad Nacional del Sur (PGI 24/Q061) is gratefully acknowledged; S.T. and P. dP are Fellows of the CONICET; M.A.F. is Researcher Fellow of the CONICET Argentina. We also thank M. Sánchez for her language assistance in the editing process.

References

[1] C.T. Moynihan, Solid State Ion. 105 (1998) 175–183.
[2] J. Ross Macdonald, J. Appl. Phys. 107 (2010) 101101–101109.
[3] P.B. Macedo, C.T. Moynihan, R. Bose, Phys. Chem. Glasses 13 (1972) 171–179.
[4] V. Provenzano, L.P. Boesch, V. Volterra, C.T. Moynihan, P.B. Macedo, J. Am. Ceram. Soc. 55 (1972) 492–496.
[5] P.E. di Prátula, S. Terny, E.C. Cardillo, M.A. Frechero, Solid State Sci. 49 (2015) (83 e 89).
[6] R.D. Shannon, Acta Crystallogr. A 32 (1976) 751–767.
[7] E.C. Cardillo, S. Terny, M.A. Frechero, Thermochim. Acta 566 (2013) 10–14.
[8] N.H. Ray, J. Non Cryst. Solids 15 (3) (1974) 423–434.
[9] B. Roling, Dielectr. Newsl. (November 2002) 1–5.
[10] F.I. Rhouma, A. Dhahri, J. Dhahri, M. Valente, Appl. Phys. Mater. Sci. Process. 108 (2012) 593–600.
[11] K.L. Ngai, J. Phys. Condens. Matter 15 (2003) 1107–1125.
[12] C.S. Terny, E.C. Cardillo, P.E. diPrátula, M.A. Villar, M.A. Frechero, J. Non Cryst. Solids 387 (2014) 107–111.
[13] S. Terny, M.A. De La Rubia, S. Barolin, R.E. Alonso, J. De Frutos, M.A. Frechero, Bol. Soc. Esp. Ceram. Vidrio 53 (1) (2014) 15–20.
[14] S. Terny, M.A. De la Rubia, R.E. Alonso, J. de Frutos, M.A. Frechero, J. Non Cryst. Solids 411 (2015) 13–18.
[15] S. Terny, M.A. De la Rubia, J. De Frutos, M.A. Frechero, J. Non Cryst. Solids 433 (2016) 68–74.
[16] A. Dutta, T.P. Sinha, P. Jena, S. Adak, J. Non Cryst. Solids 354 (2008) 3952–3957.
[17] K.J. Rao., Structural Chemestry of Glasses, 1°ed. Elsevier, 2002 (ISBN 0–08–043958-6).
[18] R.A. Gerhardt, J. Phys. Chem. Solid 55 (1994) 1491–1506.
[19] C.T. Moynihan, L.P. Boesch, N.L. Laberge, Phys. Chem. Glasses 14 (1973) 122–125.
[20] M.V.N. Sharma, A.V. Sarma, R.B. Rao, Turk. J. Phys. 33 (2009) 87–100.
[21] J.R. Macdonald, J. Appl. Phys. 84 (2) (1998) 812–827.
[22] B.V.R. Chowdari, R.G. Krishnan, S.H. Goh, K.L. Tan, J. Mater. Sci. 23 (1988) 1248–1254.
[23] A. Ghosh, A. Pan, Phys. Rev. Lett. 84 (2000) 2188–2190.
[24] S. Szu, S.-G. Lu, Physica B 391 (2007) 231–237.
[25] K.J. Moreno, A.F. Fuentes, M. Maczka, J. Hanuza, U. Amador, J. Santamaría, C. León, Phys. Rev. B 75 (2007) 184303–184308.
[26] E. Cardillo, R. Montani, M.A. Frechero, J. Non Cryst. Solids 356 (50–51) (2010) 2760–2763.
[27] M. Ingram, B. Roling, J. Non Cryst. Solids 265 (2000) 113–119.
[28] M. Garza-García, J. López-Cuevas, C. Gutiérrez-Chavarría, J. Redón-Angeles, J. Valle-Fuentes, Bol. Soc. Esp. Ceram. Vidrio 46 (3) (2007) 153–162.
[29] M. Grofmeier, F.V. Natrup, H. Bracht, Phys. Chem. Chem. Phys. 9 (2007) 5822–5827.
[30] G.N. Greaves, S. Sen, Adv. Phys. 561 (2007) 1–166.
[31] D.L. Sidebottom, B. Roling, K. Funke, Phys. Rev. B 63 (2000) 024301–024307.
[32] D.L. Sidebottom, J. Phys. Condens. Matter 15 (2003) 1585–1594.
[33] D.L. Sidebottom, Phys. Rev. B 71 (2005) 134206–134207.